International Journal of Thin Films Science and Technology

http://dx.doi.org/10.18576/ijtfst/110117

Modelling and Digital Mapping of the Infiltration Characteristics of Major Agricultural Soils

Abdel-rahman A. Mustafa [1], *Gomaa A. M. Ali* [2] *and Mahdy H. Hamed* [3,*]

[1]Soil and Water Department, Faculty of Agriculture, Sohag University, Sohag, Egypt
[2]Chemistry Department, Faculty of Science, Al-Azhar University, 71524, Assiut, Egypt
[3]Soil and Water Department, Faculty of Agriculture, New Valley University, New Valley, Egypt

Received: 1 Sep. 2021, Revised: 8 Nov. 2021, Accepted: 2 Dec. 2021.
Published online: 1 Jan. 2022.

Abstract: A study was attempted to assess the infiltration characteristics of major soils of Sohag governorate, Egypt. Twelve soil profiles were exposed and morphologically examined to represent the soils of the study area. Horizon-wise soil samples were taken and analyzed for physical and chemical properties. The infiltration field measurements were made for five hours using a double-ring infiltrometer, and the empirical Kostiakov's infiltration model was applied. The results indicated that the soils were classified as Aridisols, Entisols, and Vertisols. Initial infiltration rates ranged between 0.80 and 6.67 m/day. The highest values (6.47 and 6.67 m/day) were observed in locations No. 11 and 12, where the coarse texture prevailed. The fine texture soils recorded the lowest values (0.80, 0.81, and 0.82 m/day) in locations No. 8, 4, and 7, respectively. Infiltration rate is classified as very rapid, rapid, moderately rapid, and moderate. A correlation was found between steady infiltration rates and sand, hydraulic conductivity, $CaCO_3$ content, and organic carbon in order r=0.95, 0.93, 0.74, and 0.79. However, were found to be negatively correlated with the infiltration rates (r= -0.80, -0.91, -0.95, -0.97, -0.64, -0.91, respectively. Whereas bulk density showed an insignificant relationship (p=0.05) with infiltration rates in the order of r=0.13. GIS environment was used to generate different maps of soil parameters, and finally, the infiltration map was produced for the study area.

Keywords: Modelling, Digital Mapping, Infiltration Characteristics, Agricultural soils.

1 Introduction

Water is one of the critical factors limiting crop growth in arid and environments, especially under arid and semi-arid conditions [1, 2]. Several environmental problems are created with the rapidly increasing population, including groundwater quality deterioration. Under these areas, acceptable water management practices are needed for solving irrigation-related problems. The downward movement of water into the soil is known as infiltration, and the rate at which it occurs is defined as the infiltration rate [3]. It depends on the soil properties such as hydraulic conductivity, soil texture, initial moisture content, porosity, and organic matter [4]. The soil survey staff classifies infiltration rates into seven groups varying from rapid to very. GIS and remote sensing (RS) technology have extensively effortlessly evaluated environmental resources. In groundwater studies, GIS and RS are ordinarily used to study different groundwater objectives.

Dagadu and Nimbalkar measured the basic infiltration rates of different soils in Sangola, district solapur of the Maharashtra region [5]. The obtained results indicated that the basic infiltration rate of black cotton compact soil 1.2 cm/h, black cotton ploughed soil 1.6 cm/h, black cotton harrowed soil 1.46 cm/h, and sandy soil 8.53 cm/h. The infiltration rate of unploughed and ploughed clay was 1.2 cm/h and 1.6 cm/h, respectively. They found that Horton's model is the best fit, whereas the Green – Ampt model fits ploughed clay soil.

The soil organic matter, bulk density, specific gravity, initial soil moisture, soil type, and porosity are the crucial factors influencing infiltration rate [6-8]. The obtained results showed two infiltration rates i.e. very-fast infiltration (45.10 cm/h) and fast infiltration (17.70 cm/h). Uloma et al., 2014 determined the Ikwuano-Umuahia soils' infiltration model parameters by applying the empirical kostiakov's infiltration model [9, 10]. They found that the infiltration rate varied from 0.02 cm min^{-1} to 0.88 cm min^{-1}. Another study assessed the Harari region's infiltration characteristics of Zimbabwe's reclaimed soils [11]. The results indicated that the studied soils were characterized as loamy sand to clay loam texture, nonsaline, and non-alkali. The soils can be classified as moderate to moderately rapid. Thus, this study assessed and

*Corresponding author E-mail: mahdy.hamed@agr.nvu.edu.eg

© 2022 NSP
Natural Sciences Publishing Cor.

mapped the infiltration characteristics of Sohag Governorate, Egypt's main agricultural soils. The obtained data is important for the sustainable management of water resources.

2 Experimental Section

2.1 The study area

Sohag governorate (Fig. 1) covers a part of the Nile Valley, Egypt, and extends from the northern side of Qena governorate at latitude 26°07′N to the southern side of Assiut governorate at latitude 26°57′N. It is bounded between longitudes 31°20′ and 32°14′E.

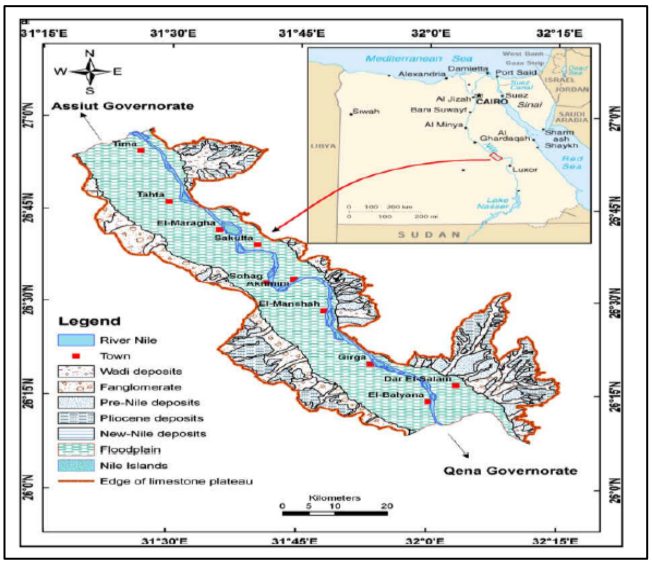

Figure 1. Location of the study area.

As stated by the Census estimation in 2019, the total population in Sohag reached 5 (10^6) people [12, 13]. They represent about five percent of the Egyptian population. The area's economy depends chiefly on crop production, namely, wheat, cotton, sugar cane, corn, sorghum, and other crops. The study area is generally characterized by hot summer and mild winter with low rainfall and high evaporation (Figs. 2 and 3).

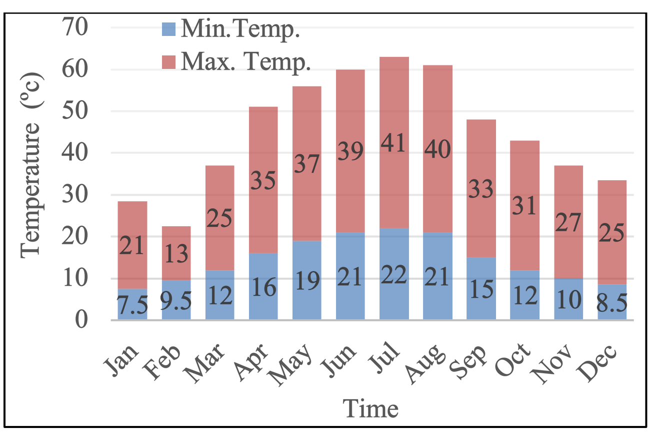

Figure 2. The temperature in the study area.

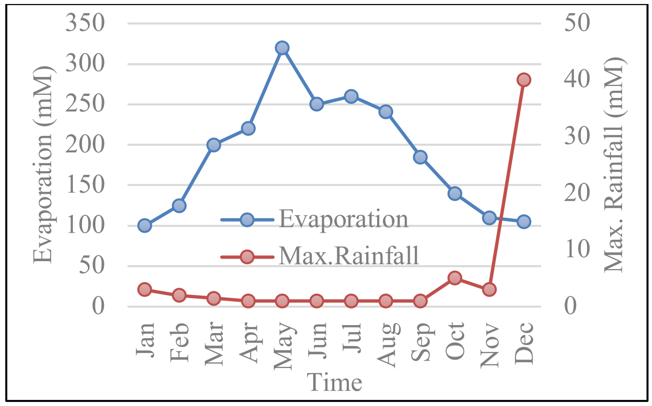

Figure 3. Mean evaporation and rainfall in the study area during 2018-2019.

2.2 Remote sensing data

The present study used the Landsat ETM+ satellite data of 2018. The study area is covered by three images viz., (175Path /42 Row, 176 Path /42 Row, and 176 Path /41 Row). The digital data of geo-coded cloud free of three images were downloaded from http://glcf.umd.edu/data/landsat/. The ASTER data was used to prepare a DEM and slope map of the study area (Figs. 4 and 5) with a spatial resolution of 15-m following the procedure elaborated by Hirano et al. (2003). The land use cover map (Fig. 6) was also generated [14].

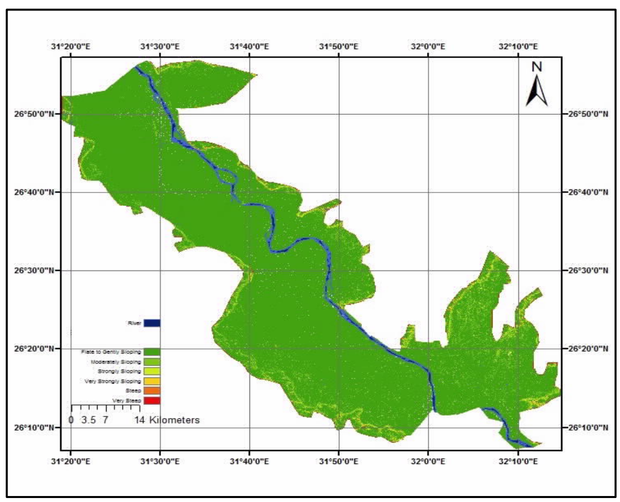

Figure 4. The slope map of the study area.

© 2022 NSP
Natural Sciences Publishing Cor.

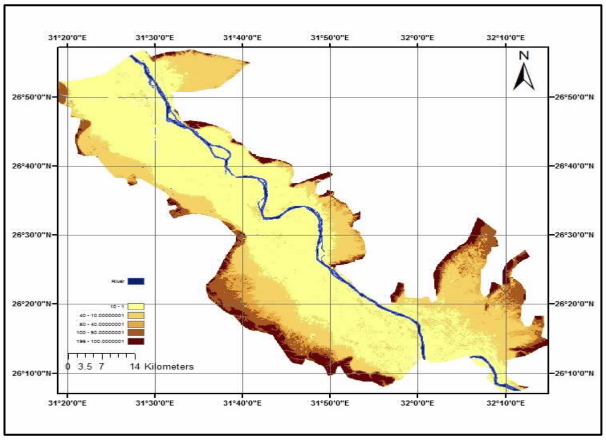

Figure 5. The digital elevation model (DEM) map of the study area.

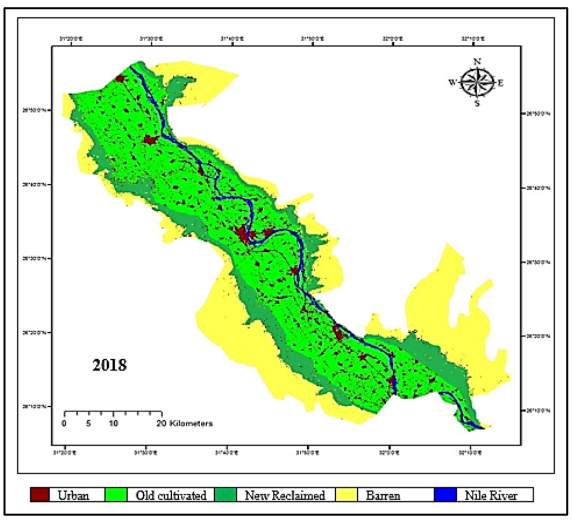

Figure 6. Land use and land cover map of the study area.

2.3 Methodology

The method followed in this study is presented in Fig. 7.

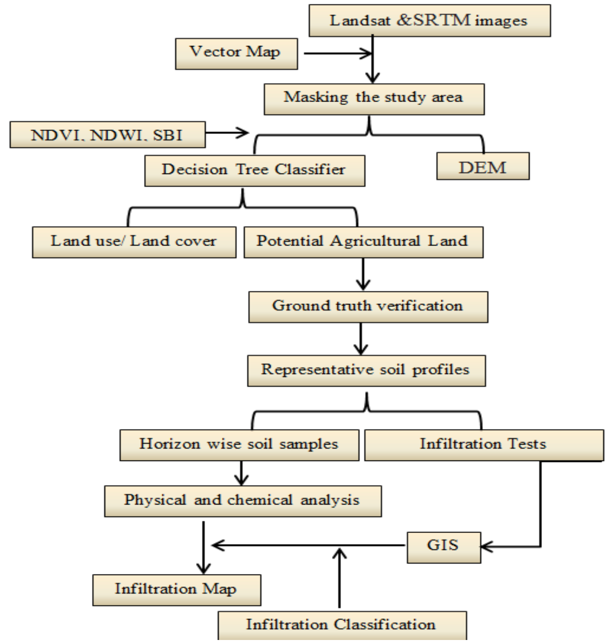

Figure 7. Flow chart of the methodology followed in this study.

2.4 Pre-processing of remote sensing data

Essential steps were done before DIP (digital image processing). This includes the generation of false-color composite images (FCC), mosaicking of the three images, and sub-image extraction through on-screen digitization of the area of interest (AOI) and masking out (Fig. 8) using subset module of ENVI software (ver.4.8).

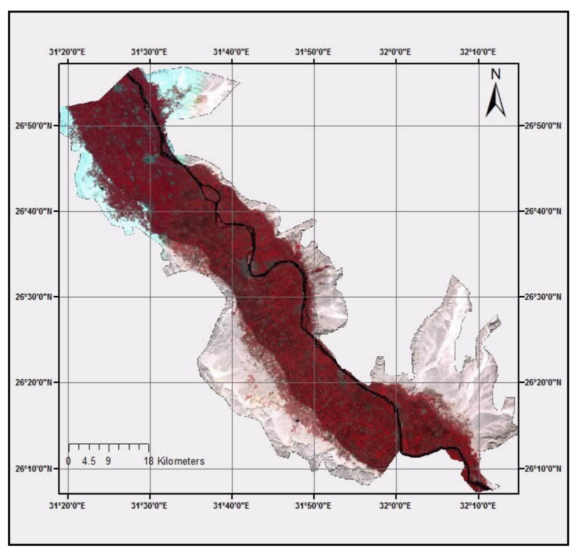

Figure 8. FCC of the study area.

2.5 Spectral indices

Three different spectral indices were used in the present study to recognize various targets. The main spectral indices used were NDVI (Normalized Difference Vegetation Index), NDWI (Normalized Difference Water Index), and (SBI) Soil Brightness Index.

2.6 Classification approaches

A decision tree classifier (DTC) is a hierarchically based classifier i.e., a data set containing (ω) themes are classified into successive levels of lesser complexity till each class is separated (Fig. 9).

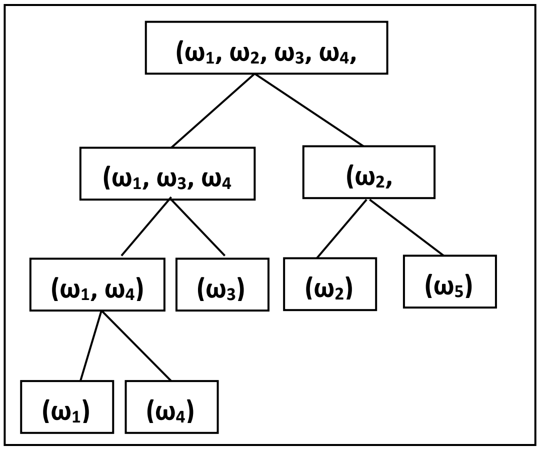

Figure 9. Example of a binary tree (ω: specific class).

2.7 Soil samples collection

Twelve representative soil profiles were selected from different mapping units. Consequently, the morphological examination of these profiles was done according to FAO guidelines [15]. In addition, disturbed soil samples (Fig. 10) have been collected and analyzed following the methods elaborated [16].

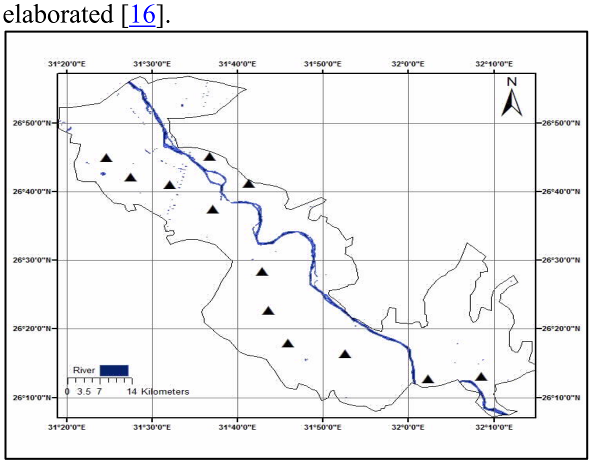

Figure 10. Location of the selected soil profiles.

2.8 Soil Taxonomy

The American Soil Taxonomy [17] was followed to classify the different soils of the studied area up to the sub great group level (Fig. 11).

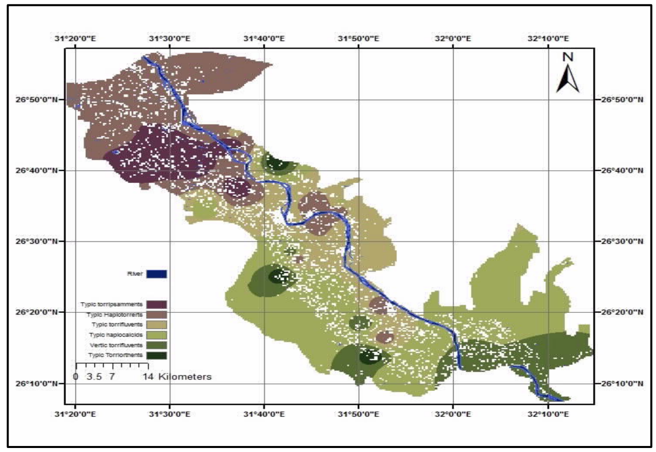

Figure 11. Soils of the study area.

2.9 Infiltration rates measurements

Three infiltrometer tests were measured at the sites using double rings at intervals of 1, 2, 5, 10, and 20 minutes, and minutes and after 300 minutes, the constant rate was obtained. The steady infiltration rate (I) in cm min^{-1} and cumulative infiltration (i) in cm as a function of elapsed time (t) in min were approximated by Kostiakov's equation [10]. The infiltration rates were classified according to Kohnke classification [18].

2.10 Generation of thematic maps

The obtained data were imported into a GIS database. The spatial analyses function in Arc-GIS 10 was used to generate the thematic map of infiltration rate.

2.11 Statistical analysis

The statistical software package STATISTICA Version 7 was employed to analyze data.

3 Results

The first zone is represented by two soil profiles, namely 11, and 12 whose properties are shown in Table 1. The sandy textural class is prevailing in this zone in which the field capacity (FC) was 9.89 and 8.1%, whereas the permanent wilting point (PWP) varied from 4.4 and 4.1% for profiles No. 11 and 12, respectively. Consequently, the available water was low, having values of 5.49 and 4 % for the two profiles (11 and 12, respectively). Also, the hydraulic conductivity (HC) was rapid for both profiles. Regarding the chemical soil properties, the soils were nonsaline, very low to low content of organic carbon (OC), low for both exchangeable cation capacity (CEC) and exchangeable sodium percentage (ESP) [19]. On the other hand, the $CaCO_3$

© 2022 NSP
Natural Sciences Publishing Cor.

% was high for both profiles, indicating these soils' calcareous nature. The infiltration rate (IR) (Table 2) revealed that IR is nearly similar within the soil profiles and classified as a moderate infiltration class. The values of IR (Figs. 12 and 13) were 6.47 and 6.67 m/day for profiles No. 11 and 12, respectively. Furthermore, the values of cumulative infiltration rate were 3534.5 and 3589.3 cm.

The second zone is represented by five soil profiles of sandy (profiles No. 1 and 5) to sandy loam (profiles No. 6, 9, and 10) texture. As the soil texture is of paramount importance for influencing other soil properties, there was a clear distinction between the second zone profiles. The sandy texture profiles (i.e., profiles No. 1 and 5) have similar FC, PWP, and HC values. On the other hand, profiles No. 6, 9, and 10 were relatively heavy textured (sandy loam) and had greater FC and PWP values but fewer HC values. Consequently, the first two profiles displayed a high IR of 5.04 and 5.78 m/day compared to soil profiles No. 6, 9, and 10, with relatively lower IR values of 3.83, 3.69, and 3.66 m/day. Hence, the soil IR of this zone was rated as rapid. The cumulative infiltration rate values were 3340.1, 3489.2, 2645.6, 2499.7, and 2508.5 cm for profiles No. 1, 5, 6, 9, and 10, respectively. Concerning the chemical soil properties, the soils were nonsaline, very low to the low content of organic carbon (OC), and low for both exchangeable cation capacity (CEC) and exchangeable sodium percentage (ESP). On the other hand, the $CaCO_3$ % was high for profiles No. 1 and 5, but low for the other profiles indicating the former mentioned soil profiles' calcareous nature.

Only profile No. 2 was considered a third zone representative with a sandy-clay texture. The tabulated data cleared that the FC and PWP were 32.4 and 22.12 %. The HC was 2.14 mm/h, classified as slow permeability. The soils were nonsaline, with low OC content, CEC, ESP, and $CaCO_3$ content. The IR was considered moderately rapid with a value of 2.82 m/day. The value of the cumulative infiltration rate was 4460.1 cm.

Finally, profiles No. 3, 4, 7, and 8 (the most heaver texture among other profiles) represent the fourth zone. This zone's soils have the highest FC values, PWP, and available water but the lowest HC records. Additionally, the soil profiles were nonsaline except profile No. 3, slightly saline. This zone's soil profiles observed the most significant OC, CEC, and ESP values. Inversely, the soils were noncalcareous. The IR values were classified as a middle class and could be arranged in 1.06, 0.82, 0.81, and 0.80 m/day for profiles No. 3, 7, 4, and 8. Consequently, the cumulative infiltration values were 1315.4, 1335.1, 1352.8, and 1312.3 cm for the same order as the former profiles (Table 3 and Fig. 14).

Table 1. Physical properties of soil profiles.

Location No.	Sand %	Silt	Clay	Texture	PWP %	FC	BD g/cm^3	AW %	HC mm/h
1	88.70	5.80	5.50	s	3.22	10.98	1.30	7.76	104.61
2	55.65	7.86	36.49	sc	22.12	32.40	1.54	10.27	2.14
3	42.67	29.33	28.00	cl	25.27	39.52	1.37	14.25	11.2
4	40.57	15.61	43.83	c	27.85	38.54	1.45	11.90	0.90
5	88.60	4.93	6.47	s	7.18	12.19	1.39	5.01	99.75
6	61.07	20.87	18.07	sl	13.46	23.60	1.43	10.13	35.12
7	26.21	27.86	45.93	c	27.43	40.35	1.37	12.92	1.26
8	29.46	21.59	48.95	c	29.21	41.62	1.38	12.41	0.67
9	75.00	13.17	11.83	sl	9.95	17.50	1.67	7.55	29.57
10	74.46	14.03	11.51	sl	10.01	17.87	1.70	7.86	28.08
11	83.29	9.83	6.88	s	4.40	9.89	1.51	5.49	120.78
12	91.73	3.41	4.86	s	4.10	8.10	1.43	4.00	129.02

PWP: Permanent Wilting Point; FC: Field capacity; BD: Bulk Density; AW: Available water; HC: Hydraulic Conductivity

Table 2. Chemical properties of soil profiles

Location No.	ECe dS/m	pH	OC %	CEC Cmol+/kg	ESP %	$CaCO_3$ %	Classification
1	0.31	7.90	0.14	5.19	3.39	10.59	Typic Torripsamments
2	0.47	7.81	0.35	8.44	8.07	4.77	Typic Haplotorrerts
3	3.65	8.54	0.58	11.72	17.13	4.91	Typic Torrifluvents
4	0.89	7.88	0.55	10.98	9.43	4.40	Vertic Torrifluvents
5	1.94	7.70	0.41	3.12	8.15	19.16	Typic Haplocalcids
6	1.98	7.82	0.29	4.03	5.02	1.78	Typic Haplotorrerts
7	0.89	7.62	0.58	17.43	46.93	4.96	Vertic Torrifluvents
8	0.51	7.77	0.79	18.05	40.07	3.00	Vertic Torrifluvents
9	0.32	7.96	0.32	6.55	1.50	0.78	Typic Torripsamments
10	0.28	8.01	0.38	7.10	1.41	0.62	Typic Torripsamments
11	0.45	8.00	0.39	2.52	7.39	21.13	Typic Haplocalcids
12	1.20	8.05	0.08	2.25	5.36	33.94	Typic Torriorthents

© 2022 NSP
Natural Sciences Publishing Cor.

ECe: Electrical conductivity of soil paste; OC: Organic carbon; CEC: Cation Exchangeable capacity; ESP: Exchangable Sodium Percentage.

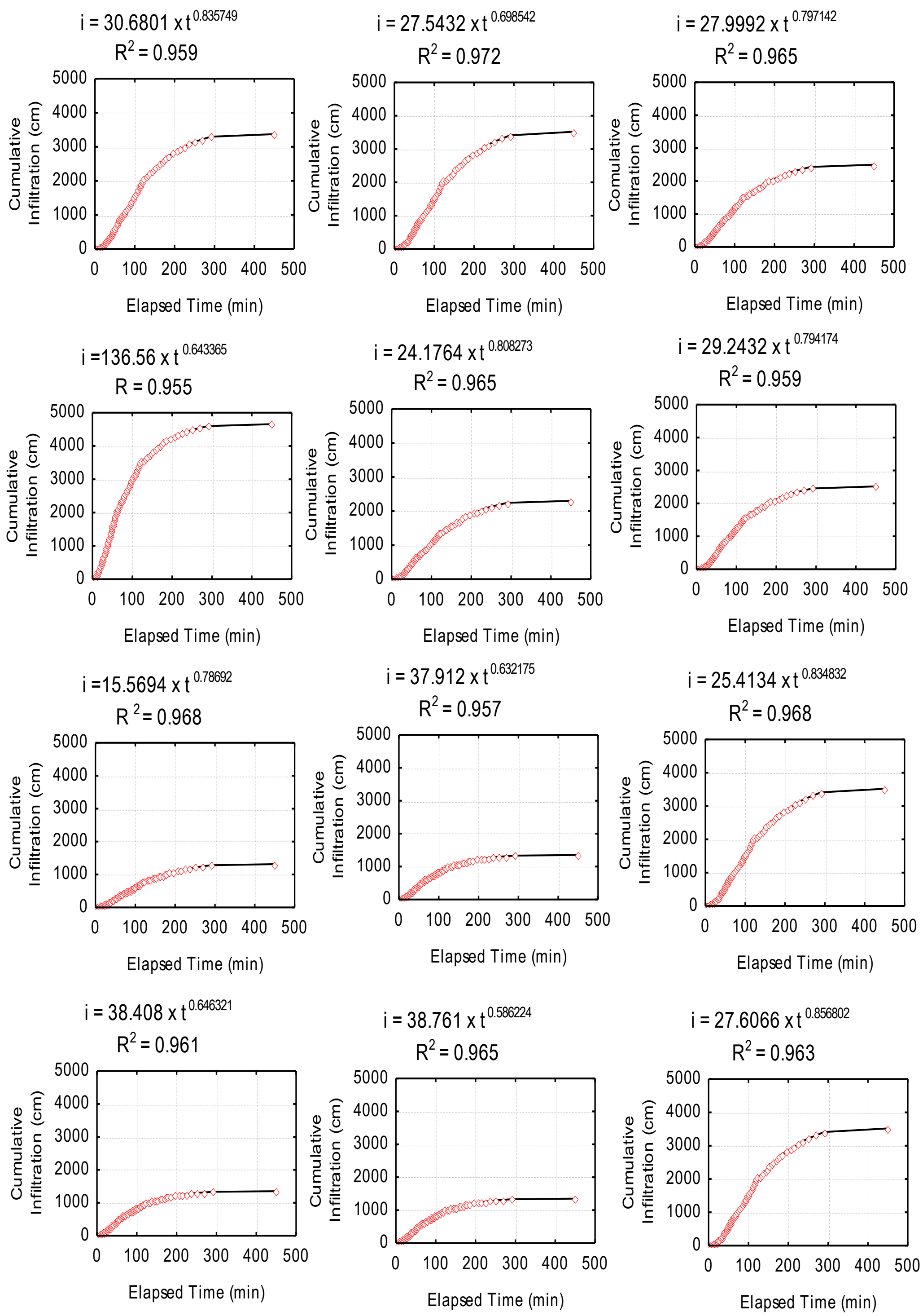

Figure 12. Infiltration characteristics (cumulative infiltration) of the soil profiles.

© 2022 NSP
Natural Sciences Publishing Cor.

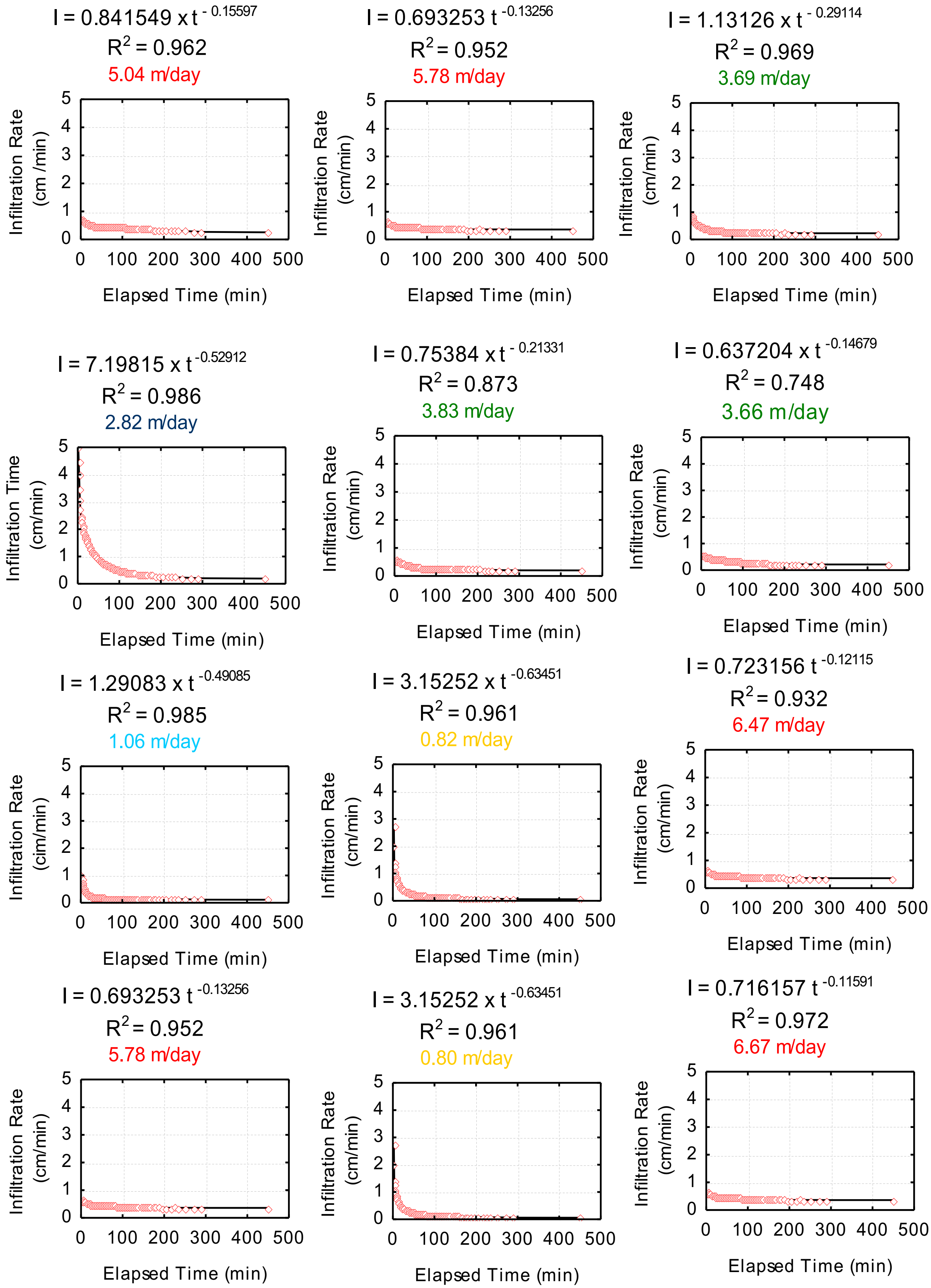

Figure 13. Infiltration characteristics (infiltration rate) of the soil profiles.

© 2022 NSP
Natural Sciences Publishing Cor.

Table 3. Classification of IR and the suitability of soils for surface irrigation.

Site No.	IR m/day	IR cm/h	Classification of IR
1	5.04	21.00	Rapid
2	2.82	11.75	Moderately Rapid
3	1.06	4.42	Moderate
4	0.81	3.38	Moderate
5	5.78	24.08	Rapid
6	3.83	15.96	Rapid
7	0.82	3.42	Moderate
8	0.80	3.33	Moderate
9	3.69	15.38	Rapid
10	3.66	15.25	Rapid
11	6.47	26.96	Very Rapid
12	6.67	27.79	Very Rapid

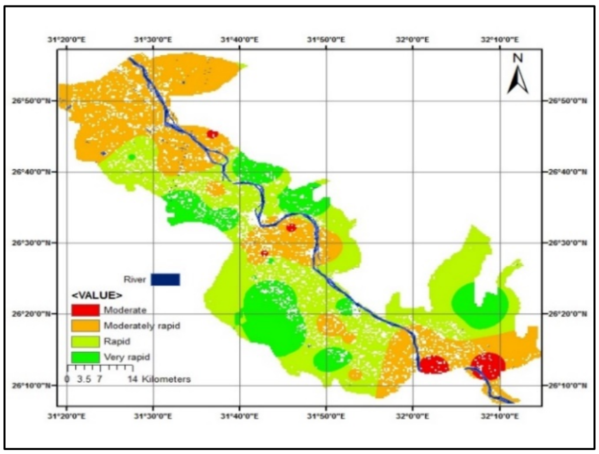

Figure 14. IR of the studied soils.

Table 4 illustrates the relationship between infiltration rate IR and soil properties. The results indicated a highly significant positive correlation between sand %, HC, and $CaCO_3$ % in the studied soil profiles and their IR. On the other hand, there was show a highly significant negative correlation.

Table 4. The relationship between infiltration rate IR and soil properties.

Soil properties	Correlation coefficient	The regression equation
Sand	0.95**	IR= -2.143 + 0.08868 * Sand
silt	-0.80**	IR= 6.4013 - 0.2029 * silt
Clay	-0.91**	IR= 6.0741 - 0.1172 * Clay
OC	-0.79**	IR= 7.0254 - 8.837 * OC
HC	0.93**	IR= 1.5475 + 0.04064 * HC
$CaCO_3$	0.74**	IR= 1.9858+0.16018 * $CaCO_3$
PWP	-0.95**	IR= 6.6334 - 0.2071 * PWP
FC	-0.97**	IR= 7.4202 - 0.1627 * FC
ESP	-0.64*	IR= 4.6704 - 0.0948 * ESP
CEC	-0.91**	IR= 6.4745 - 0.3722 * CEC
BD	0.13	IR= 0.01559 + 2.3532 * BD

4 Discussion

Efficient water management required greater infiltration control to help solve many problems such as upland flooding, pollution of surface and groundwater, declining water tables, inefficient and uniform irrigation of agricultural lands, and wastage of water [20]. As clear from obtained results, different soil properties affect its infiltration rate characteristics. According to IR viz, the soils of the study area were classified into five zones, very rapid, rapid, moderately rapid, and moderate. The infiltration rates are influenced by the initial moisture content, surface condition, hydraulic conductivity of the soil profile, texture, porosity, degree of swelling of soil colloids, organic matter, vegetative cover, duration of irrigation or rainfall, and viscosity of water [21]. However these, soil texture plays a predominant role [22]. Management practices such as tillage, by their ability to vary the topsoil composition, also influence infiltration. The coarse texture soil has the highest infiltration rate.

The variation of infiltration rate with changes in the soil texture has been investigated, and it was found that a high level of dependence of infiltration rate on the soil fine fraction [23]. This was observed in the high R2 value obtained from the regression analyses. Also, the variations of IR may be due to different land use and management types. The value of soil infiltrability under different drylands types has been estimated, and it was found that the highest infiltration rate occurs in lowland rainfed (rainfed sawah landuse) and the lowest rate of infiltration on the dryland (Tegalan landuse) [6]. Soil infiltrability was influenced by rainfall, vegetation type, soil water content, and soil characteristics. Soil properties that affect infiltration are soil structure, texture, soil organic matter content, bulk density, particle density, and initial soil moisture content. In the same trend, the constant infiltration rates of different soils under different soil conditions and their results found that the values of infiltration models vary from soil to another also the soil condition also affects the infiltration rate [5]. Finally, the hydraulic properties of the soil are influenced by many physical and chemical factors, the majority of which are difficult to measure and almost impossible to control. Both spatial and temporal infiltration variability is present within fields. Some of this variation can be linked to observable soil factors, while much remains unexplained [24].

5 Conclusions

A study was attempted to assess the major Soils of Sohag Governorate, Egypt. Different maps of soil parameters have been generated under GIS environment, and finally, the infiltration map has been produced for the study area. At the same time, the fine texture soils recorded the lowest values. Infiltration rate is very rapid, rapid, moderately rapid, and moderate. There were strong relationships between steady infiltration rates and hydraulic conductivity, $CaCO_3$ content, and sand. Silt, clay, organic carbon (OC), permanent wilting

© 2022 NSP
Natural Sciences Publishing Cor.

point (PWP), field capacity (FC), exchangeable sodium percentage (ESP), and exchangeable cation capacity (CEC), however, were found to be negatively correlated with the infiltration rates. In comparison, the bulk density (BD) showed an insignificant relationship with the infiltration rate. Different maps of soil parameters have been generated under GIS environment, and finally, the infiltration map has been produced for the study area. These obtained data are important for the best irrigation management practices in the study area.

References

[1] A. Wild, Soils and the Environment, Cambridge University Press1993.

[2] H. Hag Husein, B. Lucke, R. Bäumler, W. Sahwan, A Contribution to Soil Fertility Assessment for Arid and Semi-Arid Lands, *Soil Systems*, 5(3) 42, 2021.

[3] G.E. Osuji, Water storage, water use and maize yield for tillage systems on a tropical alfisol in Nigeria, *Soil and Tillage Research*, 4(4) 339-348, 1984.

[4] K.E. Saxton, W.J. Rawls, J.S. Romberger, R.I. Papendick, Estimating Generalized Soil-water Characteristics from Texture, *Soil Sci. Soc. Am. J.*, 50(4) 1031-1036, 1986.

[5] J.S. Dagadu, P. Nimbalkar, Infiltration studies of different soils under different soil conditions and comparison of infiltration models with field data, *International Journal of Advanced Engineering Technology*, 3(2) 154-157, 2012.

[6] I.W. Ayu, S.P. Soemarno, I.I. Java, Assessment of infiltration rate under different drylands types in Unter-Iwes subdistrict Sumbawa Besar, Indonesia, J*ournal of Natural Sciences Research*, 3(7) 2013.

[7] Y. Kim, S. Jeong, J. Kim, Coupled infiltration model of unsaturated porous media for steady rainfall, *Soils and Foundations,* 56(6) 1071-1081, 2016.

[8] T.D. Schowalter, Decomposition and Pedogenesis, in: T.D. Schowalter (Ed.), Insect Ecology (Second Edition), Academic Press, Burlington, 2006, pp. 405-435.

[9] A. Uloma, A. Samuel, I. Kingsley, Estimation of Kostiakov's Infiltration Model Parameters of Some Sandy Loam Soils of Ikwuano – Umuahia, Nigeria, *Open Transactions on Geosciences*, 2014(1) 34-38, 2014.

[10] A.N. Kostiakov, On the dynamics of the coefficient of water percolation in soils and the necessity of studying it from the dynamic point of view for the purposes of amelioration, *Trans. Sixth Comm. Int. Soc. Soil Sci.*, 1 7-21, 1932.

[11] G. Abdel Rahman, A.M. Talaat, C. Zawe, Assessment of infiltration rate for sustainability of Reclaimed area in Harare region-Zimbabwe, *Middle East Journal of Agriculture Research*, 5(1) 1-5, 2016.

[12] H. Sayed, Egypt's demographic opportunity: preliminary assessment based on 2017 census, Cairo: UNFPA/Egypt and CAPMAS, 2018.

[13] M. El Sayed, Integration of Remote Sensing & GIS to Manage the Sustainable Development in the Nile Valley desert fringes of assiut-sohag governorates, upper Egypt, *Journal of the Indian Society of Remote Sensing,* 44(5) 759-774, 2016.

[14] A.E.-R.A. Mustafa, A.R. Moursy, Integration of geoinformatics and ahp model for soil site suitability analysis for the major crops in Sohag, Egypt, *International Journal of Recent Advances in Multidisciplinary Research,* 7(7) 5784-5796, 2020.

[15] R. Jahn, H. Blume, V. Asio, O. Spaargaren, P. Schad, Guidelines for soil description, FAO2006.

[16] N.R.C.S. United States Department of Agriculture, Soil Soil Survey Investigations Report, No. 42, Version 4.0, 2004.

[17] N.R.C.S. United States Department of Agriculture, Keys to Soil Taxonomy, Natural Resources, Conservation Service (NRCS), Eleventh Edition., 2010.

[18] H. Kohnke, Soil physics soil scientist. Purdue Univ, TATA. Mc Graw Hill. Publishing company Ltd., New Delhi. India, 1980.

[19] L. Ding, P. Rangaraju, A. Poursaee, Application of generalized regression neural network method for corrosion modeling of steel embedded in soil, *Soils and Foundations*, 59(2) 474-483, 2019.

[20] M. Rashidi, A. Ahmadbeyki, A. Hajiaghaei, Prediction of soil infiltration rate based on some physical properties of soil, *American-Eurasian Journal of Agricultural & Environmental Sciences*, 14(12) 1359-1367, 2014.

[21] J. Xue, K. Gavin, Effect of rainfall intensity on infiltration into partly saturated slopes, *Geotechnical and Geological Engineering*, 26(2) 199, 2008.

[22] D. Rao, M. Manna, An Appraisal of Soil Quality Assessment Indicators In Abrol IP et al (Eds). Conservation Agriculture-Status and Prospects, Proc. National Conference on Conservation Agriculture: Conserving Resources-Enhancing Productivity. CASA, New Delhi, 2005, pp. 210-217.

[23] F. Adeniji, B. Umara, J. Dibal, A. Amali, Variation of infiltration rates with soil texture. A laboratory study, *International Journal of Engineering and Innovative Technology*, 3(2) 454-459, 2013.

[24] F. Haghnazari, H. Shahgholi, M. Feizi, Factors affecting the infiltration of agricultural soils, International *Journal of Agronomy and Agricultural Research*, 6(5) 21-35, 2015.

© 2022 NSP
Natural Sciences Publishing Cor.